

A Novel Tomographic Flow Analysis System

Andrew Hunt¹, John D Pendleton¹ and Robert B White²

¹Tomoflow Ltd, West Hembury Farm, Askerswell, Dorchester DT2 9EN, UK enquiries@tomoflow.com

²CSIRO Minerals, Clayton, Australia

ABSTRACT

A novel flow analysis system is described which uses twin-plane tomographic data to derive detailed pictures of the velocity and concentration structure within complex two-phase flows. Initial results have been obtained using electrical capacitance tomography (ECT) but other modalities may also be used. By defining a set of contiguous zones over the flow cross-section the full integration of flowrate may be undertaken and a mass flowmeter created for two-phase systems. A number of flows have been analysed, and detailed results from selected tests are presented. The simplest experiments consist of solid particles dropped under gravity through a 50mm diameter pipe, which approximates the conditions at the exit of an industrial storage hopper. More complex flows were generated in a recirculating flow rig and are typical of conditions in an industrial pneumatic conveying line. The ECT flow analysis results can be used to explore the detail of complex structures and velocity fields while comparisons with computational fluid dynamics models, high-speed video and other measurements show that the ECT results are consistent and accurate to within a few per cent of the true value.

Keywords multiphase flow, tomography, velocity, mass flowmeter, computational fluid dynamics

1 INTRODUCTION

From its first beginnings, process tomography was aimed at providing multiphase flow rate measurements as well as pictures of concentration distribution (Salkeld 1991, Hayes 1994). Measurement of flowrate through tomography demands accurate images of concentration, high-speed data acquisition, high-speed processing and some method of measuring velocity. Flowmeters for industrial use must also be robust and low-cost. Electrical Capacitance Tomography (ECT) has always offered one of the best chances of achieving the necessary compromises to become an industrial flowmeter since, although it is a low-resolution system, the sensors are simple and the acquisition rates are in principle only limited by the time to establish the electric field. Although acquisition and processing were initially seriously limited by computing speed, commercial ECT systems are now available which can produce twin-plane images with real-time image capture and reconstruction at up to 300 complete frames per second (Byars & Pendleton 2003). The interpretation of ECT images can successfully characterise the performance of two-phase flow systems comprising a non-conducting continuous phase. Such systems include major commercial applications such as pneumatic conveying of solids, many flow mixtures within the oil industry and gas-solid fluidised beds, where it has been found that the concentration distribution at the boundary of the rising bubbles depends on the properties of the bulk solid (White, 2001).

Cross-correlation has often been used as a means of measuring velocity, and commercial flowmeters are available (Beck and Plaskowski 1987). Cross-correlation within two-phase flows has a major advantage – the contrast between the two-phases tends to be high, giving plenty of structure on which to correlate; but a major disadvantage – the correlation is essentially the square of the signal, so within any volume the largest signal changes, and hence the largest flow structures, dominate the result. Sensors which average across the entire flow cross section give results which are entirely dependent on the flow structure and which cannot be reliably interpreted without knowledge of that structure (Lucas 1987). This limitation does not stop the application of cross-correlation in multiphase flow measurement (Thorn, Hammer and Johansen 1999) but can seriously restrict the range of operating conditions where reliable answers can be obtained. Cross-correlation of sub-sections of image planes reduces this volume averaging effect and approaches closer to the true integral of concentration and velocity. Several authors have undertaken these calculations with reasonable results (e.g. Jaworski and Dyakowski 2001). Non-axial velocities may be estimated through cross-correlation of pixels or groups of pixels within the same or separate planes (eg. Mosarov et al 2002).

This paper presents a software package we have written to give the researcher a flexible tool to investigate multiphase flows using ECT. Within this package many of the techniques suggested by

other researchers have been implemented, and new techniques may easily be assimilated as they become available. In addition to providing a flow research tool, the ECT flow analysis package can be used to address many of the outstanding questions that must be addressed before commercial tomographic flowmeters can be produced.

2 EQUIPMENT AND DATA ANALYSIS

The results presented here were obtained using a Tomoflow R100 ECT flow analysis system, comprising pipe-mounted sensor, data acquisition module, and control computer with real-time and off-line flow imaging and analysis software (Figure 1). The capacitance measurement unit is the high-speed design with embedded PC as described by Byars and Pendleton (2003).

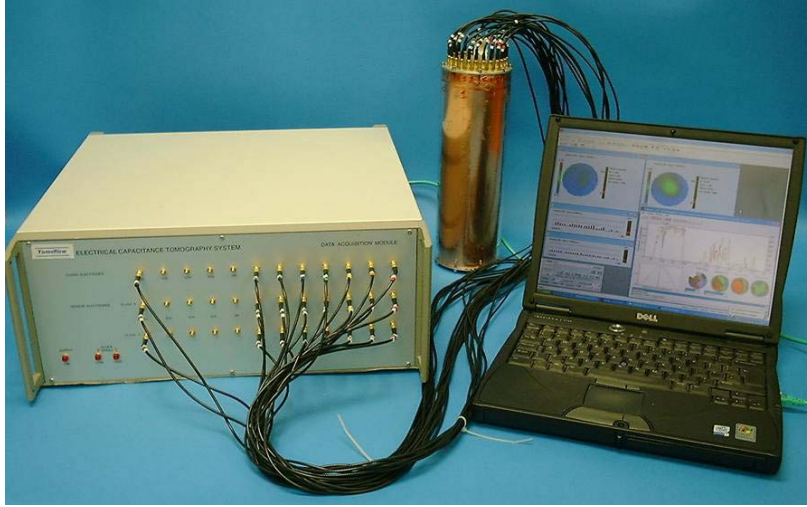


Figure 1. Tomoflow R100 Flow Analysis System

Twin-plane sensors are used in conjunction with guard electrodes to create two image 'planes' axially separated along the flow. Each 'plane' is in fact a cylinder of finite length made up of 812 pixels on a 32x32 square. Images of flows are shown here as circular maps with a grid of 32x32 pixels using a colour scale from black (pixel full of low permittivity material) to white (pixel full of high permittivity material). To investigate details of flow conditions it is more helpful to divide each image plane into a number of zones arranged appropriately for the flow conditions. For 8 electrode systems, dividing the flow into 13 zones as shown in Figure 2 gives zones containing approximately 62 pixels each and which have typical length scales of $D/2$ axially and $D/4$ within the cross section where D is the pipe diameter. These zones are more consistent with the linear spatial resolution of ECT which is sometimes quoted as D/n_e where n_e is the number of electrodes circumferentially around the pipe. Within each zone the pixel values are averaged to give one concentration value per zone for each frame of data. An example (the centre zone of 13) of the resulting time-concentration plots is shown in Figure 3.



Figure 2. Typical 13-zone division of circular flow section derived from pixel grid

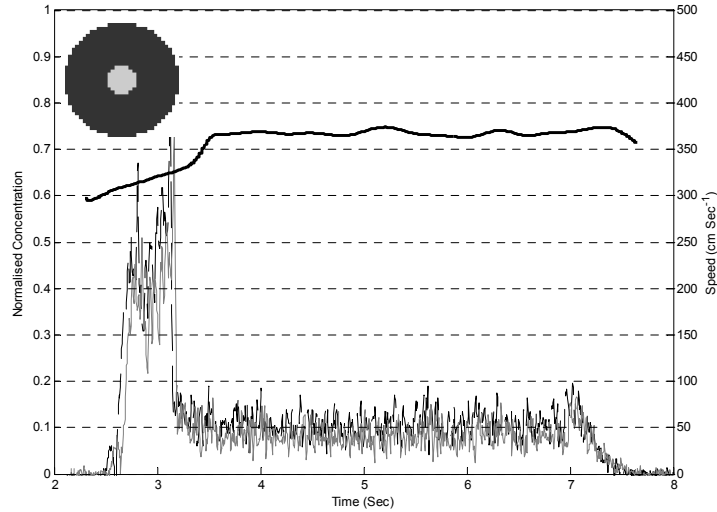


Figure 3. Graph of concentration against time (left-hand scale) and velocity against time (right-hand scale) for gravity drop flow in centre zone. Dashed line is concentration in 1st plane, light grey line is concentration in 2nd plane, black line is velocity. Results are plotted from centre zone of 13 zones.

The velocity at each point in time within each zone is calculated by correlating the instantaneous concentration of one plane with the same zone in the other plane. The result is plotted as a second graph with axes in cm/second on the right hand side of the graph. The correlation process is described mathematically as:

$$R_{xy,i}(\tau) = \lim_{T \rightarrow \infty} \frac{1}{T} \int_0^T C_{1,i}(t) C_{2,i}(t + \tau) dt \quad (1)$$

where $C_{1,i}(t)$ and $C_{2,i}(t)$ are the instantaneous concentrations in zone i in plane 1 and 2 respectively. Although mathematically the correlation is described for the averaging time T approaching infinity, in practice the velocity will fluctuate over some much shorter time scale and the user will need to set the window T at some suitable value appropriate to the particular length and velocity scales in the flow and the sensor geometry.

The resulting correlogram has a clearly discernible peak if the flow structures are coherent over the sensor length (Figure 4) and contains information about the time domain statistics of the flow – primarily convection and dispersion. The simplest assumption is that the time delay at the peak of the correlogram corresponds to the transit time of flow structures between the two planes. The peak may be found by the greatest single value, centre of area or polynomial fitting. For these types of gravity particle flows we find polynomial fitting gives the most consistent results though all the other techniques are available in the software. The time window used for the correlation process needs to be shaped in some way to minimise artefacts caused by sharp-edged windows. This shaping is known as apodization and various apodization functions are programmed into our software – the results presented here use the common Hanning window, which is a smooth bell shape.

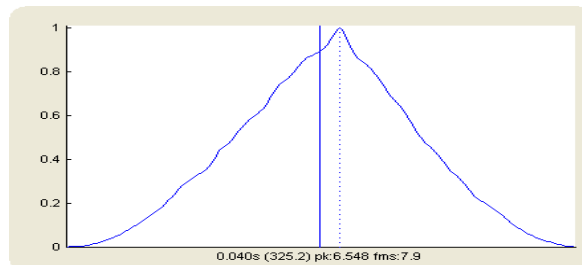


Figure 4. Normalised correlogram R_{xy} corresponding to marked time point in Figure 3. Horizontal axis is delay time, which at correlogram peak is 0.04 seconds, equivalent to 7.9 frames of data.

If $\tau_i(t)$ is the time delay at the correlogram peak for zone i at each frame at time t , then the transit velocity is given by:

$$V_i(t) = S / \tau_i(t) \quad (2)$$

where S is the separation distance between the centre of the sensor electrodes. The volumetric flow per zone is given by:

$$q_i(t) = V_i(t) \cdot C_i(t) \cdot A_i \cdot \Delta t \quad (3)$$

where Δt is the time interval between successive frames and A_i is cross-sectional area of each zone. $C_i(t)$ is in this case taken as the average of $C_{1,i}(t)$ and $C_{2,i}(t)$. The total volume flowing between time t_1 and t_2 can then be calculated as:

$$Q = \sum_{t=t_1, t_2} \sum_{i=1, n} q_i(t) \quad (4)$$

The concentrations $C_{1,i}(t)$ and $C_{2,i}(t)$ are instantaneous averages over a volume corresponding to $A_i \times L_s$ where L_s is the sensor electrode length. The velocity $V_i(t)$ is an average over a volume $A_i \times (L_s + S)$ and also a time average over the correlation window T . The volumetric flowrate $q_i(t)$ is an average over the volume $A_i \times (L_s + S)$ and also a rolling average over T updated at each time frame Δt , q is often expressed in industrial situations as a 1 second value. The flow volume Q is integrated over the time period between time t_1 and t_2 and may be visualised as the equivalent to volume measurement through filling a tank over a time period.

3 FLOW EXAMPLES

3.1 Gravity-drop flow

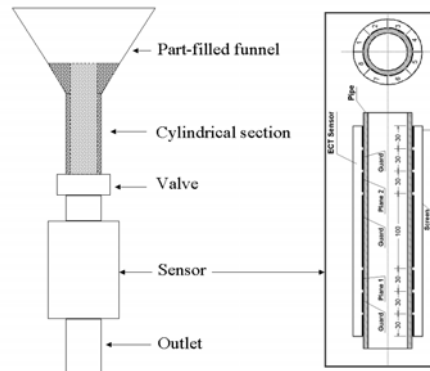


Figure 5. Gravity drop flow-rig schematic with detail of sensor on right

A simple gravity-drop flow is used to illustrate the level of detail that can be obtained from ECT-based flow measurement. A funnel and cylindrical pipe of 0.0495m diameter were part-filled with a measured volume of plastic beads (Figure 5). The beads are retained by a ball valve above an ECT sensor connected to a Tomoflow R100 flow analysis system as previously shown in Figure 1. The sensor is the same as reported for the tests of Jaworski and Dyakowski (2001). The ECT system had been calibrated by filling successively with air and then beads to give a concentration range from 0 to 1. When the valve is opened the beads pass under gravity from the funnel through the sensor and outlet. Figure 3 shows the concentration and velocity against time for the central zone of the 13 zone map from Figure 2 for a typical test with data acquisition of 200 frames per second. Figure 6 shows the cross-sectional images for the two image planes at a various times, the first time of 3.126 seconds is marked by the cursor on Figure 3. It can be seen from these figures that after the valve is opened, a dense plug of beads falls down the centre of the pipe between about 2.5 seconds and 3.2 seconds. The transit time of the last 'spike' of concentration in the upper plane at 3.126s can clearly be seen to arrive at the lower plane at 3.171s – a delay corresponding to the correlogram peak at 0.04 seconds

within the frame rate resolution of .005s. Following this a trickle of beads continues for another 4 seconds or so until the funnel is empty.

The velocity of the plug starts at about 2.8m/s rising to about 3.7m/s. This speed increase is consistent with the fact that the lowest beads fall about 0.4m before arriving at the upper plane of the sensor, while the upper beads fall about 0.7m. The beads falling from the funnel after the first plug show a steady velocity of about 3.7m/s and though barely discernible in the pictures of concentration distribution (Figure 6) the signals correlate well between the two planes (Figure 3).

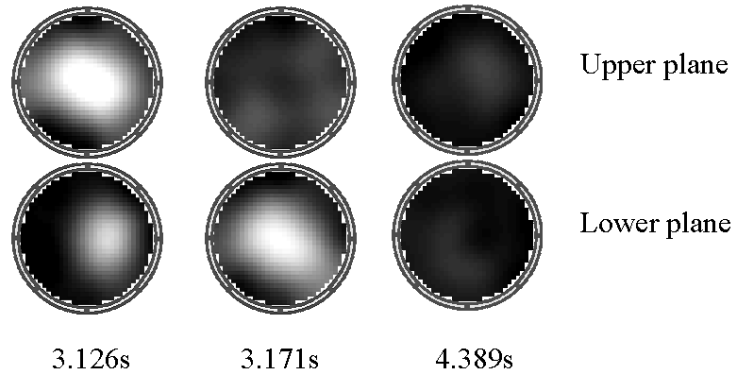


Figure 6. Images at various times from the gravity-drop flow test. White represents solids, black is air.

Integrating the whole flow period between 2s and 8s gives an estimate of volume of 2.335 litres, compared to the actual value of 2.379 litres – within 2%. The plug between 2.5 and 3.2 seconds can be separately integrated and shows a volume of 0.591 litres. This plug volume corresponds to a cylinder of 0.0495m diameter and 0.307m length, which is the cylinder of beads from the top of the valve to the top of the beads within the part-filled funnel (as shown in lighter grey in Figure 5). It appears then that as the valve is opened the entire volume of the cylinder of beads supported by the valve, both in the cylindrical section and within the funnel, drops as one accelerating mass down through the centre of the sensor. The remaining beads within the funnel then trickle out in the manner of an egg-timer at a much lower rate. An understanding of this type of behaviour will assist in the design of industrial hoppers or silos where many types of solids may be difficult to discharge.

3.2 Pneumatic conveying

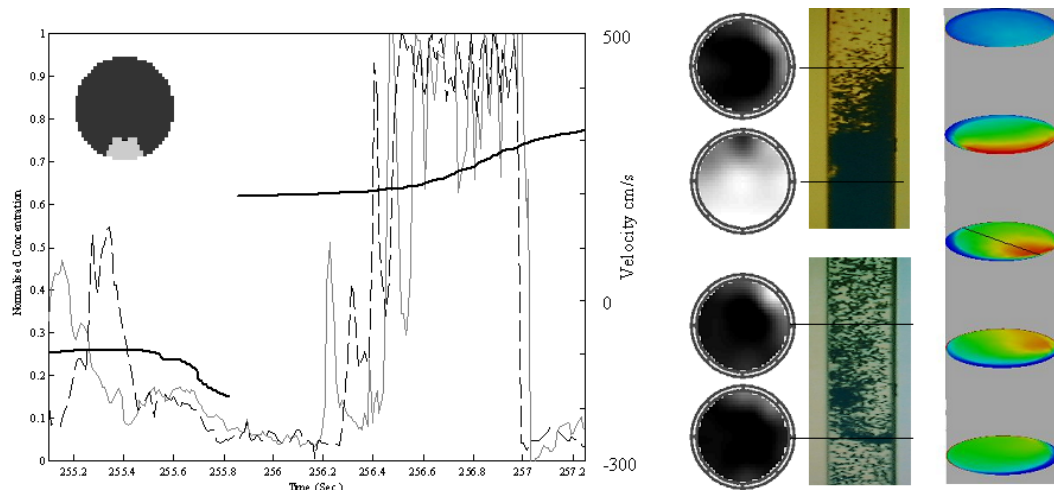


Figure 7. Pneumatic conveying. Graph shows concentration (left-hand scale) and velocity (right-hand scale, cm/s) for zone shown. Light grey line is upper plane concentration, dashed grey line is lower plane. Velocity is the dis-jointed black line (dotted section is downflow, solid section is upflow). Circular ECT images (black is air, white is solids) shown with still frames from high-speed video pictures of flow and cross-section concentration plots from CFX output.

Figure 7 shows the concentration and velocity plots for an upward flow of plastic beads at an average rate of 900 kg/hr blown by air at a superficial velocity of 2.6 m/s in a 50mm ID pipeline, as described by Jaworski and Dyakowski (2001) where ECT was used as part of an EU-funded CRAFT project. Also shown are stills from high-speed video and cross-sectional images from the ECT system. The same flow conditions have been modelled using a commercial computational fluid dynamics package, CFX5.5.1, and some concentration cross-sections are shown for comparison. Detailed analysis of the various outputs shows that the flows are highly complex with upflow and downflow alternating in time, even though the average flow is upwards. Frequently during the period marked 'downflow' the solids are falling down the pipe in 'ropes' around the outside of the pipe, often with up and downflow simultaneously at different physical locations. This type of behaviour is also seen in the two-phase, Eulerian - Eulerian CFD model. ECT images and our zoned velocity calculations give a much clearer measure of the location and velocity than simple 2-D side-view high-speed video. A future paper will explore the use of ECT for validation of computational models, and indeed ECT offers one of the few experimental techniques capable of producing 3-D output for comparison with computation in multiphase flows.

4 CONCLUSIONS

We have described a flow analysis system based on ECT where the flow can be divided up into a number of user-defined zones. Within each zone the concentration against time can be viewed and correlation can be undertaken to establish the transit velocity at each point in time within each zone. The volumetric flowrate can be calculated for each zone by integrating concentration times velocity and the total volume passing over any period can be easily calculated. Examples from a simple gravity-drop flow have been used to demonstrate the large amount of data available from this approach, and that the integrated flow volumes are accurate to within typically about 2%. The flow analysis system can be used to investigate details of complex multiphase flows. The results can be compared with high-speed video, computational fluid dynamics calculations and integrated total flow volumes and the system forms the basis for future commercial mass flowmeters.

5 REFERENCES

- Beck M.S. and Plaskowski A. (1987) *Cross-correlation flowmeters: their design and application*, IOP Publishing, Bristol, UK.
- Byars M. and Pendleton J.D. (2003), *A new high-speed control interface for an electrical capacitance tomography system*, In Proc. 3rd World Congress on Industrial Process Tomography, Banff, Canada.
- Hayes D.G. (1994), *Tomographic flow measurement by combining component distribution and velocity profile measurements in 2-phase oil/gas flows*, PhD Thesis, UMIST, UK.
- Jaworski A.J. and Dyakowski T. (2001) *Tomographic measurements of solids mass flow in dense pneumatic conveying. What do we need to know about the flow physics?* In Proc. 2nd World Congress on Industrial Process Tomography, Hannover, Germany.
- Lucas G.P. (1987), *The measurement of two-phase flow parameters in vertical and inclined flows*, PhD Thesis, University of Manchester Institute of Science and Technology (UMIST), UK.
- Mosorov V., Sankowski D., Mazurkiewicz L. and Dyakowski T. *The 'best-correlated pixels' method for solid mass flow measurements using electrical capacitance tomography*, Meas. Sci. Technol. **13** (2002) 1810-1814.
- Salkeld J.A. (1991), *Process Tomography for the measurement and analysis of two-phase oil-based flows*, PhD Thesis, University of Manchester Institute of Science and Technology (UMIST), UK.
- Thorn R., Johansen G.A. and Hammer E.A. (1999), *Three-phase flow measurement in the offshore oil industry – is there a place for process tomography?* In Proc. 1st World Congress on Industrial Process Tomography, Buxton, UK.
- White R.B. (2001), *Gas solid contacting in a bubbling fluidised bed*, PhD Thesis, University of Melbourne, Australia